

Singlet spin order in spin pairs coupled via non-bonded interactions

Giuseppe Pileio^{1,*}, Dolnapa Yamano¹, Craig Eccles², Graham J. Tizzard³, and Sam Thompson^{1,*}

¹*School of Chemistry, University of Southampton, Southampton, SO17 1BJ, United Kingdom*

²*Magritek GmbH, Philipsstraße 8, 52068 Aachen, Germany*

³*UK National Crystallography Service, School of Chemistry, University of Southampton, Southampton, SO17 1BJ, United Kingdom*

Correspondence*:

Giuseppe Pileio and Sam Thompson

g.pileio@soton.ac.uk, st3a15@soton.ac.uk

2 ABSTRACT

3 Fluorine spin pairs that are constrained in spatial proximity show large scalar spin-spin couplings,
4 despite the atoms being separated by several bonds. This is due to a non-bonded atomic
5 interaction related to partial overlapping of fluorine p-orbitals. In this paper we exploit this
6 phenomenon to create long-lived singlet spin order on the fluorine spin pair. This form of order,
7 which, in this example molecule, is more than an order of magnitude longer than longitudinal order,
8 has the potential to be useful in magnetic resonance imaging and molecular tracing experiments,
9 because of the lack of endogenous fluorine in the human body and the high sensitivity achievable
10 in ¹⁹F NMR.

11 **Keywords:** Long-lived Spin States, Nuclear Singlet Spin Order, *Through-Space* Scalar Coupling, NMR, Fluorine NMR

1 INTRODUCTION

12 Molecular systems containing two fluorine atoms that are separated by several chemical bonds but close
13 in space, exhibit significant indirect scalar spin-spin coupling constants. In a first observation in 1956,
14 Saika and Gutowsky were surprised by the large ${}^5J_{FF} = 16$ Hz measured in $(CF_3)_2NCF_2CF_3$, where
15 the three-bond coupling was ${}^3J_{FF} \approx 1$ Hz (1) and it was common to expect a monotonic decrease
16 of the scalar coupling constant as the number of chemical bonds between the coupled atoms increases.
17 Since then the phenomenon was observed in many other systems including, saturated organic compounds
18 (2), 1-substituted 4,5-difluoro-8-methylphenanthrenes (3), 4-substituted 1,8-difluoronaphthalenes (4),
19 benzophenanthrenes (5), fluoroallyl cations (6), and difluorometacyclophanes (7, 8). The anomalous
20 size of this coupling interaction in these systems was later rationalised in terms of molecular orbital
21 theory (9) and correlated to the spatial distance between the two fluorine nuclei (10), hence the label
22 “through-space”, which is clearly improper in the NMR literature since this same label is commonly
23 used to denote the dipole-dipole interaction between spins that has a truly through-space nature. In such
24 difluoro-substituted systems, geometrical constraints give rise to a certain degree of overlap between
25 the p-orbitals (lone pairs) of the two fluorine atoms and this produces electron-filled molecular orbitals

26 with a weakly bonding (σ_{FF}) and a weakly anti-bonding σ_{FF}^* character. Despite this molecular orbital
27 configuration not leading to a net bond between the two fluorine nuclei, it results in a very effective
28 scalar coupling interaction between the two nuclear spins, effectively mediated by the four electrons in
29 those weak molecular orbitals. Since the p-orbital overlap is distance dependant, the magnitude of the
30 observed scalar coupling rapidly decays with increasing distance between the fluorine atoms. It is also
31 worth remembering that there is indeed a through bond contribution to those couplings but this is typically
32 smaller than the “through-space” one. ^{19}F - ^{19}F scalar coupling values of between 60-80 Hz have been
33 measured in substituted 1,8-difluoronaphthalene derivatives (4) and scalar coupling as large as 160-180 Hz
34 were found in substituted 4,5-difluorophenanthrene derivatives (3).

35 Systems of two scalar-coupled spin-1/2 nuclei, can be prepared to support singlet spin order, a particular
36 type of nuclear spin order that has been shown to decay much slower than longitudinal and transverse
37 magnetization, the latter two forms of spin order being used in all magnetic resonance experiments. Such a
38 slower decay has been exploited in many applications including storage of hyperpolarization (11, 12, 13),
39 investigation of weak ligand-protein binding (14), measurements of slow chemical exchange (15), small
40 diffusion coefficients (16), diffusion and tortuosity in porous media (17, 18, 19, 20, 21). Most of these
41 applications were so far based on singlet order created either in ^1H spin-1/2 pairs (because such is the
42 molecule of interest or to maximize sensitivity) or in ^{13}C - or ^{15}N -doubly enriched molecules, carefully
43 designed to maximize singlet order lifetimes. Recently, examples of singlet spin order in ^{31}P (22) and
44 ^{103}Rh spin pairs (23) were also reported.

45 In this paper, we report long-lived singlet spin order in molecules containing pairs of ^{19}F nuclei coupled
46 via non-bonded scalar interactions of “through-space” type. Accessing and exploiting singlet spin order
47 in molecules containing pairs of ^{19}F nuclei is interesting because ^{19}F has a large gyromagnetic ratio
48 (high NMR sensitivity), an essentially 100% natural abundance (no need for isotopic labelling), and
49 because there is no endogenous fluorine in living organisms. This means there is no background signal
50 in bio-medical applications, which contrasts with the intrinsic limitation in singlet NMR of molecules
51 containing ^1H pairs. However, a large chemical shift range of several hundreds of ppm’s and a typically
52 small scalar coupling¹ of molecules containing ^{19}F spin pairs (24) has not played in favour of singlet order
53 applications because this form of spin order is an **eigenoperator** of the Hamiltonian superoperator only
54 in condition of nearly-magnetic-equivalence, i.e. when the chemical shift frequency difference between
55 the two coupled nuclei is small compared to their spin mutual scalar coupling frequency. Conversely,
56 some of the systems displaying “through-space” coupling, such as substituted 1,8-difluoronaphthalenes
57 and 4,5-difluorophenanthrenes have the potential to meet the conditions for near-magnetic-equivalence,
58 capitalising on their large “through-space” coupling, which is of the order of 170-190 Hz. In addition, and
59 as exploited below, one can benefit from modern desktop NMR spectrometers and use their relatively low
60 static magnetic field (typically less than 2 T) to reduce the chemical shift frequency difference between the
61 two ^{19}F spins to meet the conditions for near-magnetic-equivalence in a larger pool of ^{19}F spin pairs, while
62 maintaining good sensitivity and high spectral resolution characteristic of these machines.

¹ The ^{19}F - ^{19}F scalar coupling can be quite large in vicinal ^{19}F pairs but then the ^{19}F nuclei are often chemically equivalent and therefore singlet order cannot be accessed.

Table 1. Sample naming, formulation and spin system parameters.

Sample	Molecule	[] (M)	J_{FF} (Hz)	$\Delta\delta_{FF}$ (ppm)
A	I	0.11	171.4	0.142
B	II	0.15	173.1	0.117
C	III	0.15	175.7	1.028

2 MATERIALS AND METHODS

63 2.1 Molecular Design, Chemical Synthesis and Characterisation

64 In seeking a molecular scaffold to support a ^{19}F spin pair of nearly-magnetic-equivalence, we speculated,
65 based on visual inspection, that molecule **I** might be a suitable candidate. Moreover, the synthetic route
66 described by Murai *et al.* (25) appeared amenable for modification such that hydrogen atoms providing
67 deleterious singlet relaxation mechanisms may be substituted with alternative groups possessing more
68 desirable magnetic properties for our purposes. Accordingly, we prepared molecule **I**, and derivative
69 molecules **II** and **III**, bearing deuterium and methoxy- d_3 groups respectively (Scheme 1). Attempts to
70 access molecule **II** by performing hydrogen/deuterium exchange on a relatively advanced precursor **4** of
71 the synthetic route to molecule **I**, *via* electrophilic substitution under acidic conditions, was unsuccessful.
72 However, treating commercially available acid **5** with the same conditions gave the trideuterobenzoic acid
73 **6** as the major isotopologue, along with small amounts of the dideutero- and monodeutero-isotopologues
74 (11 percent in each case), both as isotopomeric mixtures. Subjecting this material to the Murai synthetic
75 route provided molecule **II**. Esterification of the 3,4-difluorobenzoic acid **8** with methanol- d_4 , followed
76 by nucleophilic aromatic substitution with methanol- d_4 and DBU gave **10** as a single regioisomer in 77
77 percent yield over two steps. Again, following the route of Murai furnished molecule **III** along with a small
78 amount of the urea **11**. Vapour diffusion provided diffraction quality single crystals of both molecule **III**
79 and **11**, from which coordinates were collected ². For molecule **III**, the major occupant of the unit cell (c.
80 75 percent) has an F-F distance of 2.45 Å and the dihedral angle between the carbon fluorine bonds is 46.5
81 degrees (see supplementary information).

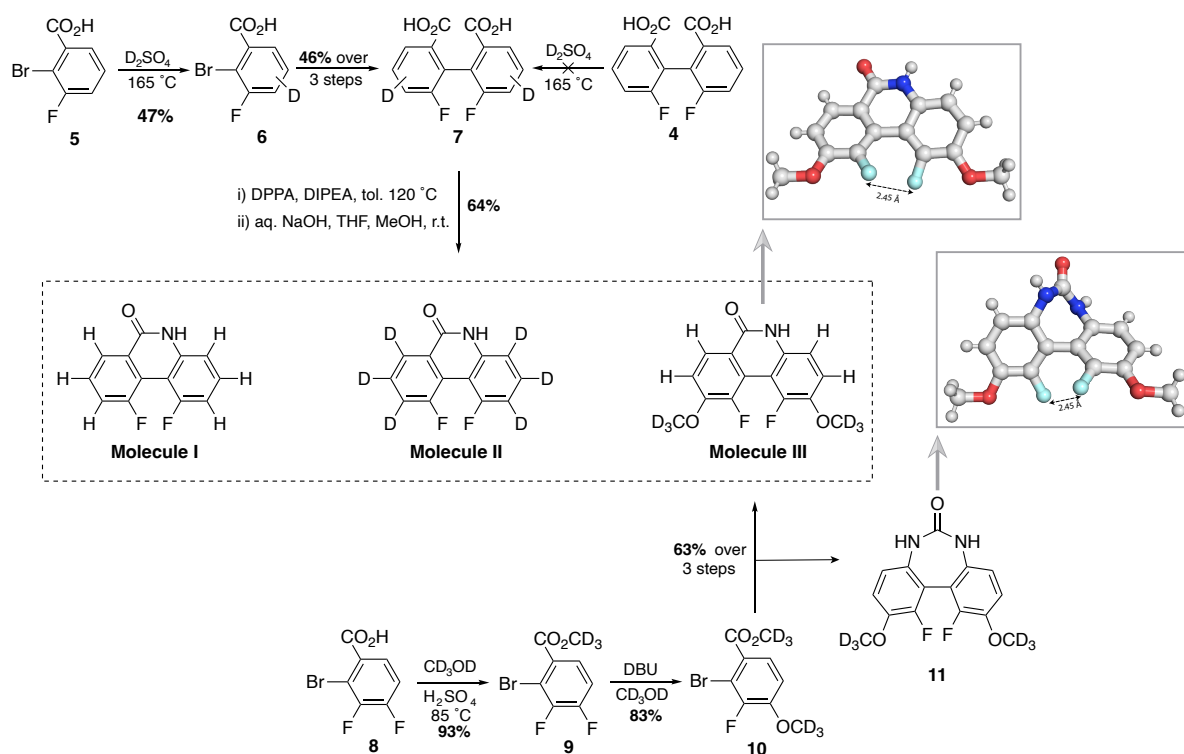
82 2.2 NMR Samples

83 Each of the three difluoro-substituted molecules **I**, **II** and **III** were dissolved in DMSO- d_6 and the solution
84 transferred into a 5 mm OD LVP J-Young valved NMR tube for the NMR experiments described below.
85 These solutions were degassed via N_2 bubbling to remove paramagnetic O_2 traces. The naming and details
86 of the three samples so prepared are reported in Table 1 together with their main spin system parameters as
87 obtained from ^{19}F and $^{19}\text{F}\{-^1\text{H}\}$ spectra.

88 2.3 NMR Experiments

89 NMR experiments were performed using two different NMR spectrometers: a 9.4 T Bruker magnet
90 coupled to an Avance II console and equipped with a selective fluorine probehead for observation of ^{19}F
91 with ^1H decoupling and z-gradients, and a 1.02 T Magritek SpinSolve 40 Carbon desktop spectrometer
92 operating at 43.4 MHz for proton. Measurements of T_1 decay constants were performed using conventional
93 inversion recovery methods (26). For the measurement of singlet order decay constants, T_S , we used the
94 methodology based on magnetization-to-singlet pulse sequence schemes described elsewhere (27) and
95 shown in Figure 1. Note that ^{19}F signal detection for Sample A and Sample C (see below) was done in the

² CCDC #2390769 (molecule **III**), #2390768 (**11**)



Scheme 1. Synthesis of molecules **I**, **II**, **III** (DBU = 1,8-diazabicyclo(5.4.0)undec-7-ene, DPPA = diphenylphosphoryl azide, DIPEA = *N,N*-diisopropylethylamine, THF = tetrahydrofuran, Me = CH₃; with x-ray diffraction data for molecule **III** and urea **11** (grey = carbon/hydrogen, blue = nitrogen, red = oxygen, cyan = fluorine).

Table 2. The parameters used to run the pulse sequence in Figure 1.

Sample	Instrument	Field (T)	τ (ms)	n_1	n_2	$\{g_1, g_2, g_3\}$ (% of max)	$\{\delta_1, \delta_2, \delta_3\}$ (ms)	τ_{90} (μ s)	τ_w^{1H} (μ s)
A	AVII-400	9.4	1.385	4	2	{15,-15,-15}	{2.4,1.4,1.0}	7.0	65.7
B	AVII-400	9.4	1.400	6	3	{15,-15,-15}	{2.4,1.4,1.0}	7.0	-
C	Spinsolve 40	1.02	1.330	7	3	{100,-100,-100}	{4,2,2}	60.0	-

96 presence of ¹H decoupling so to collapse multiplets and obtain a neater signal from which to measure the
 97 decay constant (WALTZ-90° pulse duration $\tau_w^{1H} = 65.7 \mu\text{s}$, corresponding to a nutation frequency of 3.8
 98 kHz). The measurements of T_S was done with and without a CW irradiation scheme (nutation frequency
 99 2 kHz) applied on the ¹⁹F channel during the singlet storage time (t) in order to verify the presence of
 100 relaxation through scalar coupling of the second kind mechanism.

101 The parameters occurring in the pulse sequence in Figure 1 are reported in Table 2.

3 RESULTS AND DISCUSSION

102 3.1 Sample A

103 The ¹⁹F-NMR spectrum of Sample **A**, taken at 9.4 T and 25 °C, is reported in Figure 2a and shows a
 104 complex multiplet. The spectrum is shown using a frequency scale in Hz and has been centred at 0 Hz for
 105 simplicity (the chemical shift at the centre of the multiplet is -101.7 ppm). Based on visual inspection of

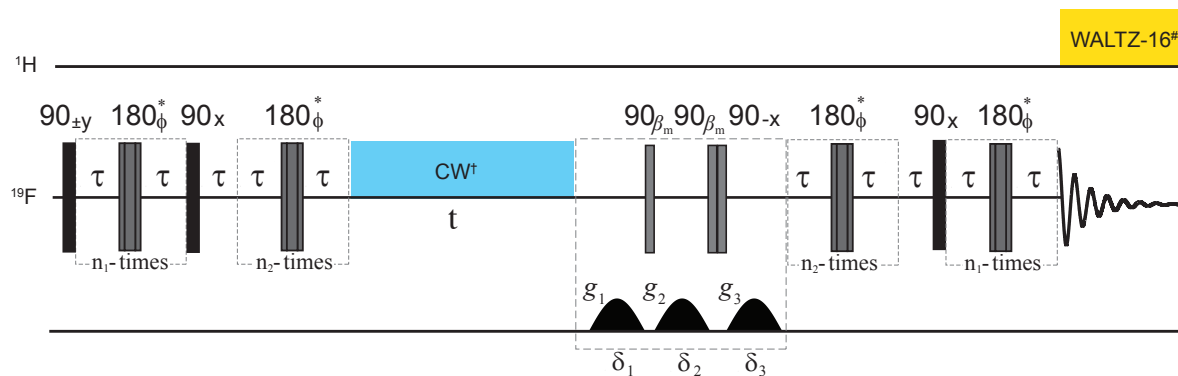


Figure 1. Pulse sequence used to measure the lifetime of singlet order in $^{19}\text{F}_2$ -enriched molecules. # WALTZ-16 decoupling during acquisition was only used for sample A and C to decouple the protons. Experiments were done with and without CW decoupling during the time interval t as described in the text. Gradients have half-sinusoidal shape on Bruker and rectangular on Magritek spectrometers. Asterisks indicate a composite 180° pulse built as $90x180y90x$. The phase ϕ is cycled as $[x,x,-x,-x,-x,x,x,-x,-x,-x,x,x,-x,-x,x]$ within the train of 180° pulses. The total echo time is $\tau_e = \tau_p + 2\tau = 1/(2(J^2 + \Delta\omega^2)^{1/2})$ where $\tau_p = 4 * \tau_{90}$ is the duration of the composite pulse and τ_{90} the duration of the 90° pulse. $n_1 = \pi J/(2\Delta\omega)$, $n_2 = n_1/2$ and $\beta_m = \arctan(\sqrt{2})$.

106 the linewidth, it is clear that the fluorine nuclei are strongly coupled to each other and weakly coupled to
 107 possibly all other protons of the aromatic rings. This is easily confirmed by the $^{19}\text{F}\{-^1\text{H}\}$ NMR spectrum
 108 of Sample A, taken at the same field and temperature (shown in Figure 2b), where a strong AB pattern
 109 is what remains of the ^{19}F peaks after proton decoupling. From the frequency value of the four peaks
 110 in Figure 2b we measured a $J_{FF} = 171.4$ Hz and a difference in chemical shift frequencies of the two
 111 fluorine atoms of $\Delta\delta_{FF} = 0.142$ ppm.

112 It is therefore clear that the ^{19}F spin pair is not isolated from the other spins in the molecule and all
 113 coupled spins should be considered in the discussion. The presence of scalar coupling to neighbouring
 114 protons may give rise to three types of problem: i) The spin Hamiltonian contains cross terms that connect
 115 the ^{19}F singlet state to the triplet states. In fact, ^{19}F singlet spin order may be not a good eigenoperator
 116 of the Hamiltonian superoperator; ii) The scalar couplings between ^{19}F and ^1H nuclei can give rise to
 117 relaxation via a scalar coupling of the second kind mechanism (S2K), which will shorten the lifetime of
 118 singlet order proportionally to the magnitude of the spin couplings involved and the size of the proton T_1
 119 decay constant (28, 29); iii) The through-space dipolar couplings to the neighbouring protons give rise to a
 120 out-of-pair dipolar coupling relaxation mechanism (oDD) that contributes, and possibly dominates, the
 121 lifetime of ^{19}F singlet order by reducing it by an extent that is proportional to the internuclear distances
 122 between ^{19}F and ^1H nuclei (30).

123 Fortunately, the large value of J_{FF} stabilises the singlet spin order between the two ^{19}F spins and ^{19}F
 124 singlet order is expected to remain a good eigenoperator of the spin Hamiltonian superoperator (31). The
 125 presence of a contribution to singlet relaxation due to scalar coupling of the second kind can be qualitatively
 126 probed (and, eventually, minimized) by applying a Continuous Wave (CW) irradiation on the ^{19}F channel
 127 (or, equivalently, on the ^1H or ^2H channel) as explained in Ref. (28). Unfortunately, the out-of-pair dipole-
 128 dipole $^{19}\text{F}\text{-}^1\text{H}$ interactions cannot be suppressed or minimised with radio-frequency-based techniques and
 129 this is likely to be the major deleterious contribution to the size of the ^{19}F singlet order lifetime in this
 130 sample. Clearly, such interactions can only be removed by chemical substitution - see below.

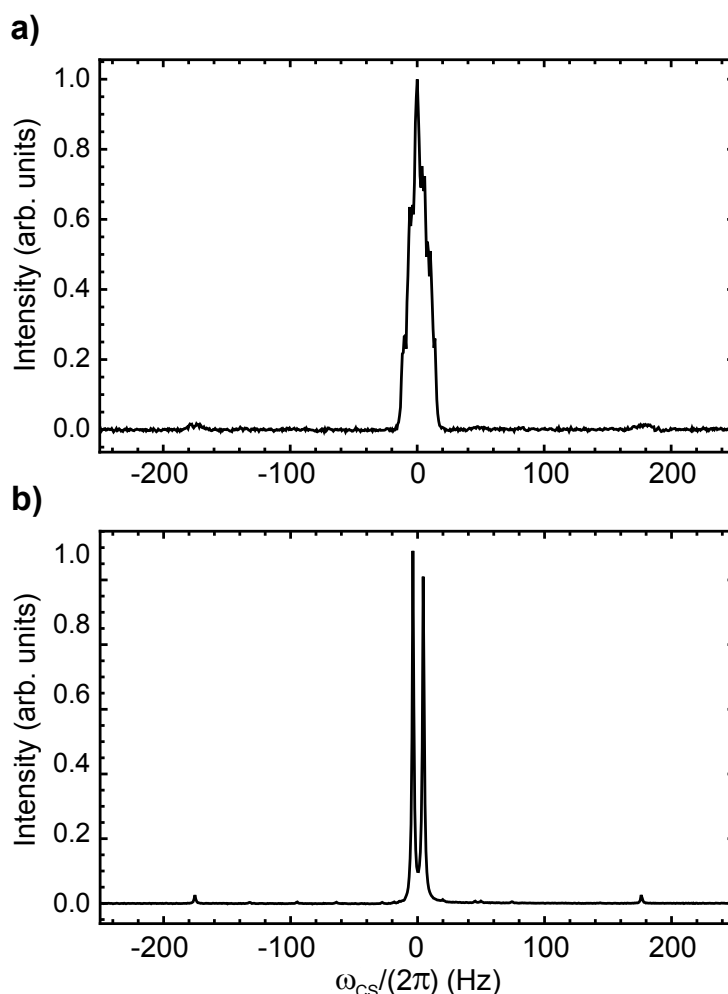


Figure 2. ^{19}F NMR spectra of Sample A taken at 9.4 T and 25 °C without (a) and with (b) proton decoupling. The intensity is in arbitrary units and the peak has been centred at 0 Hz for simplicity (the chemical shift at the centre of the multiplet is -101.7 ppm).

Table 3. The ^{19}F T_1 and T_S decay constants measured for all samples in this work. Measurements at 1.02 T were taken at 27°C while those at 9.4 T were taken at 25°C.

Sample	T_1 (1.02 T)	T_1 (9.4 T)	T_S^* (1.02 T)	T_S^* (9.4 T)	T_S^\dagger (9.4 T)
A	2.92 ± 0.23	1.26 ± 0.03	-	1.60 ± 0.05	1.65 ± 0.04
B	2.74 ± 0.17	1.34 ± 0.02	-	2.26 ± 0.03	2.31 ± 0.03
C	2.25 ± 0.11	0.48 ± 0.01	29.1 ± 2.4	$0.53 \pm 0.01^{**}$	$1.61 \pm 0.05^\ddagger$

* measured without CW irradiation during t ; † measured with CW irradiation during t .

** measured with pulse sequence in Ref. (15); ‡ measured with pulse sequence in Ref. (15) and CW irradiation on ^{19}F channel during t ;

131 With this in mind, we measured the relaxation decay constant of ^{19}F longitudinal spin order (T_1) and that
 132 of ^{19}F singlet spin order (T_S) in Sample A at 9.4 T and 25°C (data reported in Table 3). While the presence
 133 of ^{19}F singlet order is guaranteed by the singlet-filter in the pulse sequence (it only allows through singlet
 134 order) its decay constant is disappointingly short and comparable to T_1 . This is somewhat expected for the
 135 reasons explained above, i.e. because both scalar and dipolar couplings to the neighbouring protons generate

136 a significant relaxation mechanism for both T_S and T_1 . To probe the presence and importance of a S2K
 137 relaxation mechanism, we measured the singlet order decay constant T_S using the pulse sequence in Figure
 138 1, but where a CW irradiation scheme is applied during the singlet storage period (t) in order to decouple
 139 the protons from the fluorine atoms and therefore minimize an eventual S2K relaxation contribution (28)
 140 (data reported in Table 3). Since the resultant value of T_S was only marginally longer than that measured
 141 in the absence of proton irradiation (compare column 5 and 6 in Table 3), we can conclude that a scalar
 142 coupling of the second kind relaxation mechanism is not the limiting factor for the ^{19}F singlet order lifetime
 143 in sample A. It is therefore reasonable to think that the short relaxation decay constant observed for ^{19}F
 144 singlet order in Sample A is due to an oDD mechanism proportional to the size of ^{19}F - ^1H dipole-dipole
 145 couplings in the molecule. Clearly, we expect to have a contribution from chemical shift anisotropy (CSA)
 146 relaxation, a known important source of relaxation in ^{19}F -NMR spectroscopy (32), but, given the small
 147 difference between the T_1 at the two magnetic fields, this may not be the dominant one in this sample.
 148 Note that the chemical shift anisotropy mechanism acts differently on T_S than on T_1 (27) so the conclusion
 149 above can be challenged; however, it has not been possible to measure the T_S at 1.02 T for Sample A
 150 because of the large number of echoes required in the pulse sequence (due to the small chemical shift
 151 frequency difference compared to the very large scalar coupling) and the relatively short T_2 .

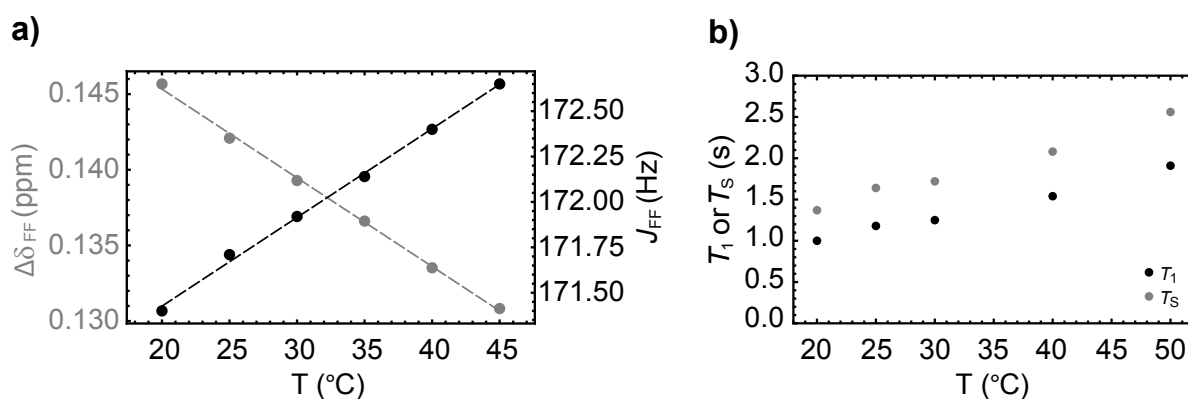


Figure 3. a) The temperature dependence of the chemical shift difference between the two fluorine nuclei (gray circles) and their mutual scalar coupling constant (black circles) in Sample A. Dashed lines are best fit to the experimental points. b) The variation of T_1 (black circles) and T_S (gray circles) with temperature measured on Sample A.

152 Given that the non-bonding nature of the ^{19}F - ^{19}F scalar coupling relies on partial orbital overlaps, we
 153 decided to explore whether the magnitude of the J_{FF} coupling depends upon temperature. To do so, we
 154 monitored the value of the ^{19}F - ^{19}F scalar coupling and the difference in chemical shift between the two
 155 fluorine nuclei over a small temperature range (see Figure 3a). We observe a small linear decrease (slope =
 156 -0.586 ppb/ $^{\circ}\text{C}$) in the chemical shift difference as the temperature is increased. Similarly, the value of J_{FF}
 157 increases linearly, but slowly, with temperature (slope = 0.05 Hz/ $^{\circ}\text{C}$). Additionally, we measured T_1 and
 158 T_S decay constants at some selected temperature values between 20 $^{\circ}\text{C}$ and 50 $^{\circ}\text{C}$, finding that both these
 159 constants increase almost linearly with temperature, although not by much (see 3b). Such a trend correlates
 160 well with the reduction in viscosity of the solvent (literature data on protonated DMSO show a reduction
 161 from 2.24 cP to 1.286 cP as the temperature is increased from 20 to 50 $^{\circ}\text{C}$).

162 **3.2 Sample B**

163 In order to remove dipolar interactions with the neighbouring proton, we synthesised molecule **II**
164 (prepared as Sample **B**, see Materials and Methods), which is an analogue of molecule **I** with the aromatic
165 ring hydrogens substituted with deuteriums so to scale down the size of the ^{19}F dipolar couplings by a factor
166 of about six (the ratio between hydrogen and deuterium gyromagnetic ratios). The ^{19}F -NMR spectrum of
167 Sample **B**, taken at 9.4 T and 25 °C, is reported in Figure 4, where a set of asterisks mark the four peaks of
168 the expected AB pattern for the two fluorine peaks in the sample (couplings to neighbouring deuterium
169 nuclei fall within the linewidth). Other than these four marked peaks, the spectrum shows a series of other
170 minor peaks that are due to the trace isotopologues containing mixtures of hydrogen and deuterium atoms
171 (see section 2.1 and supplementary information).

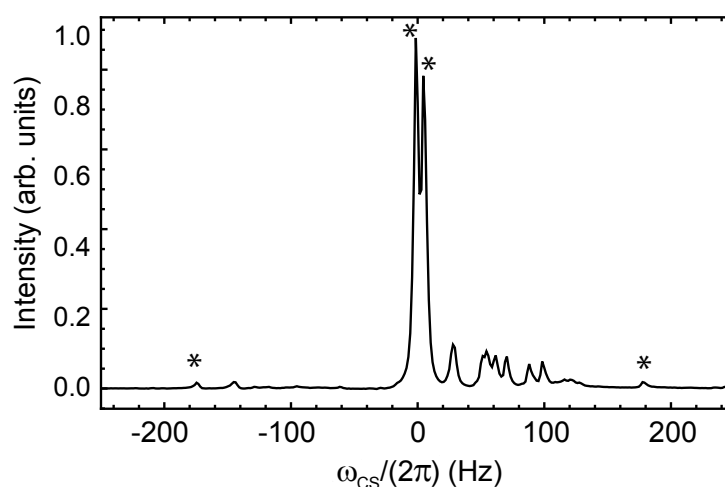


Figure 4. ^{19}F NMR spectra of Sample **B** taken at 9.4 T and 25 °C. The intensity is in arbitrary units and the peak has been centred at 0 Hz for simplicity (the chemical shift at the centre of the AB pattern is -101.8 ppm). The expected AB pattern arising from the ^{19}F spin pair is marked with asterisks. All unmarked peaks arise from isotopomers containing protons in place of deuterium.

172 A measurement of the longitudinal order decay constant at 9.4 T and 25 °C on this sample resulted in a
173 rather short value of $T_1 = 1.31 \pm 0.02$, which is only marginally longer than the one found for Sample **A**
174 (see Table 3). This is not surprising since the value of T_1 for these two samples are expected to be dominated
175 by the ^{19}F - ^{19}F dipolar interaction relaxation mechanism. Unfortunately, the measurement of the singlet
176 order decay constant in this sample, done in the same conditions and using the pulse sequence in Figure
177 1 and the parameters in Table 2, still resulted in a rather short value of T_S that is only marginally longer
178 than T_1 by a factor of 1.7 (see Table 3). These results led us to hypothesise that either the CSA relaxation
179 mechanism dominates, or in substituting hydrogens with deuteriums we may have gained by minimising
180 dipolar coupling interactions to hydrogens but reintroduced a more serious S2K mechanism. Unfortunately,
181 it has not been possible to measure the T_S of Sample **B** at 1.02 T, for the same reasons occurring in Sample
182 **A**, nor the CSA contribution can be easily calculated in absence of the full chemical shift tensors of the two
183 fluorine nuclei. Similarly, the S2K contribution depends on both the size of the scalar coupling between the
184 fluorines and the deuterons and the relaxation time of these latter nuclei (for deuterium this is dominated by
185 its quadrupolar coupling interaction) and therefore it is not easy to predict whether a deuterium is actually
186 worse than a hydrogen in the vicinity of the fluorine, as it could be the case here. Fortunately, one can

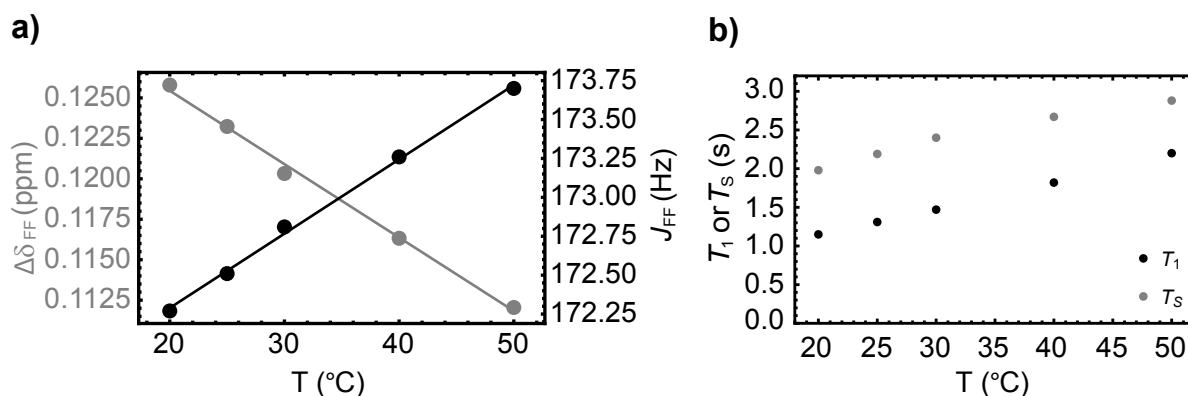


Figure 5. a) The variation with temperature of the chemical shift difference between the two fluorine nuclei (gray circles) and their mutual scalar coupling constant (black circles) in Sample **B**. Dashed lines are best fit to the experimental points. b) The variation of T_1 (black circles) and T_S (gray circles) with temperature measured on Sample **B**.

187 experimentally probe the presence of the S2K mechanism by measuring the T_S decay constant with the
 188 pulse sequence in Figure 1 and in the presence of a CW irradiation applied during the time interval t . The
 189 results, obtained with a CW nutation frequency of 2 kHz applied on the ^{19}F channel and reported in Table
 190 3, did not show an extension in T_S and therefore led us to conclude that S2K is not a limiting relaxation
 191 mechanism for Sample **B**.

192 As done for Sample **A**, we report the results of a series of experiments to study the temperature dependence
 193 of the spin system parameters (Figure 5a) and the relaxation decay constants T_1 and T_S (see Figure 5b) for
 194 Sample **B**. Similarly to what seen in the previous section, even for Sample **B** we found a slow decrease
 195 (slope = -0.454 ppb/ $^{\circ}\text{C}$) of the difference in chemical shift between the two fluorine nuclei and a slow
 196 increase in the value of the ^{19}F - ^{19}F scalar coupling (slope = 0.048 Hz/ $^{\circ}\text{C}$) as temperature is increased.
 197 Moreover, both T_1 and T_S increase slightly with temperature but this seems again consistent with the
 198 decrease in solvent viscosity over that temperature range.

199 3.3 Sample C

200 With the aim of removing any immediate nuclear spin coupled to the fluorine atoms, we synthesised a
 201 third molecule (molecule **III** in Scheme 1, prepared as Sample **C** as described in Materials and Methods)
 202 where we aimed to replace the closest spin to the two fluorine nuclei with $-\text{OCD}_3$ groups. The ^{19}F -NMR
 203 spectrum of Sample **C**, taken at 9.4 T and 25 $^{\circ}\text{C}$, is reported in Figure 6a. It consists of an AB pattern
 204 where each transition is further split into two. This is compatible with a strongly-coupled ^{19}F spin pair
 205 which is further coupled to one proton on the aromatic ring (and possibly to the other, although with a
 206 scalar coupling that falls within the linewidth). The pattern is compatible with these spin system parameters:
 207 $J_{FF} = 175.7$ Hz, $\Delta\delta_{FF} = 1.028$ ppm and $J_{FH} = 7.5$ Hz. The proton-decoupled fluorine spectrum
 208 of the same sample is reported in Figure 6b and shows the simple AB pattern expected for the proton-
 209 decoupled ^{19}F spin pair. The relatively large chemical shift difference between the two fluorine atoms
 210 corresponds to a chemical shift frequency difference of 387.2 Hz at 9.4 T. At such magnetic field, the
 211 condition $J_{FF} < \Delta\omega_{FF}$ is not met and therefore singlet order is not a good **eigenoperator** of the spin
 212 Hamiltonian anymore and an RF irradiation (33) is required in order to *lock* such form of order. Moreover,
 213 the pulse sequences in Figure 1, designed for strongly-coupled/nearly-equivalent spin pairs, performs badly
 214 at producing singlet order in this regime. For this reason the pulse sequence reported by Sarkar et al. (15)

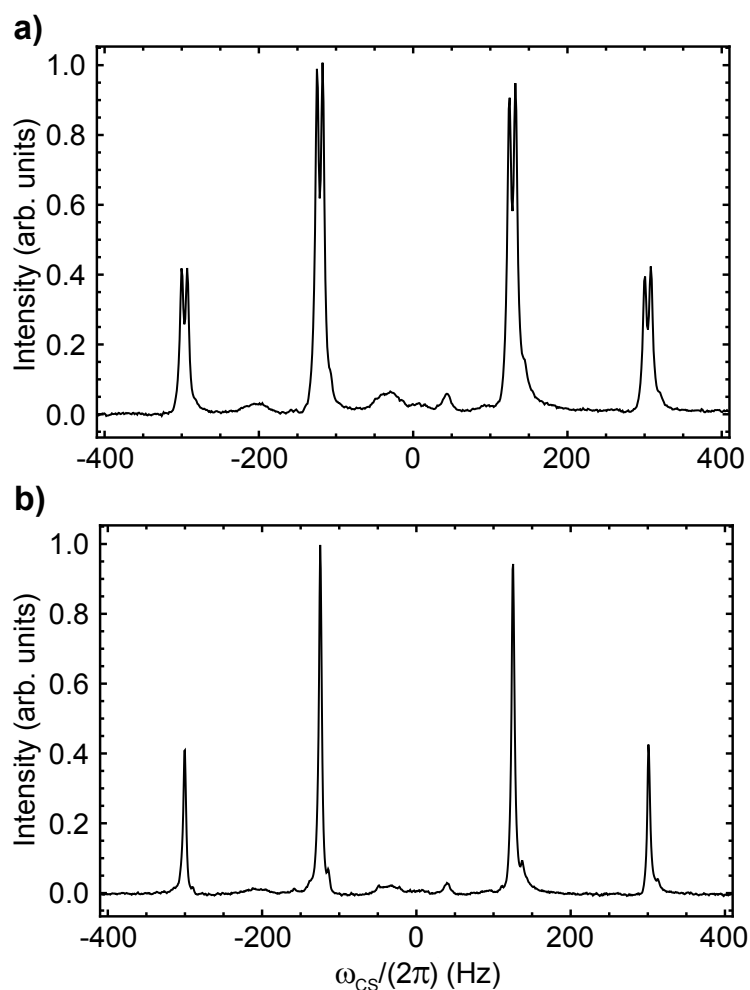


Figure 6. ^{19}F NMR spectra of Sample C taken at 9.4 T and 25 °C without (a) and with (b) proton decoupling. The intensity is in arbitrary units and the peak has been centred at 0 Hz for simplicity (the chemical shift at the centre of the multiplet is -124.6 ppm).

215 was used to measure the T_S of Sample C at 9.4 T. The resulting T_S values, reported in Table 3 with and
216 without CW irradiation on the ^{19}F channel, still show a relatively short singlet lifetime which is longer
217 than T_1 by only a factor of around three. Note the importance of the CW decoupling which is in this case
218 required because of the presence of a large chemical shift difference between the two fluorine spins (33).

219 At this point, we found it very interesting to prepare ^{19}F singlet spin order in the low magnetic field of
220 a desktop spectrometer operating at 1.02 T, where the chemical shift frequency difference is only 42.1
221 Hz and the two fluorine nuclei would remain strongly-coupled. For this, we coded the pulse sequence in
222 Figure 1 into a Spinsolve and measured both T_1 and T_S values of Sample C at 1.02 T, data reported in
223 Table 3. The value of T_1 is essentially the same as in the other two samples, again this may simply reinforce
224 the idea that T_1 in these molecules is dominated by the dipolar interaction between the two fluorine nuclei,
225 with a small contribution from CSA (34, 35, 36) (compare the values of T_1 at the two magnetic fields
226 for all three molecules reported in columns 2 and 3 of Table 3). T_S at 1.02 T, however, is appreciably
227 longer than T_1 of the same sample at the same field, and also longer than the values of T_S measured for the
228 other two samples in this paper. While there is a clear contribution from CSA in determining such a long
229 lifetime, this alone cannot justify the measured value (CSA scales with the square of the magnetic field).

230 Hence, the mechanism(s) that set the limit to the observed value of T_S are not fully clear from this set
231 of experiments and further work needs to be done in terms of experimental measurements and numerical
232 simulations. Preliminary relaxation data taken on ^1H and ^{13}C nuclei in these molecules may suggest the
233 presence of dimerization (or some other form of molecular aggregation) that, if present, would reduce
234 the molecular tumbling correlation time and therefore scale down the absolute value of both T_1 and T_S
235 achievable in these molecules. Given the nature of the scalar coupling in these systems, arising from orbital
236 overlap under steric constraints, it is also possible that scalar coupling of the first kind (S1K) plays a role in
237 determining the size of singlet relaxation decay constants.

4 CONCLUSIONS

238 We have demonstrated that the strong scalar coupling between ^{19}F spin pairs separated by many bonds,
239 but constrained in spatial proximity, can be deployed to prepare long-lived singlet spin order. In proof of
240 principle experiments conducted on three newly-synthesized molecules containing spatially-constrained
241 ^{19}F pairs that display very large scalar couplings of “through-space” nature, we have shown a 13-fold
242 extension in spin memory. **The work has evidenced a significant contribution of chemical shift anisotropy**
243 **to singlet order relaxation and hinted to the possibility of other complementary mechanisms such as scalar**
244 **coupling of the first kind or the presence of molecular aggregation. A full understanding of these relaxation**
245 **contributions requires supplementary experiments and numerical simulations that are the subject of future**
246 **work. For example, it would be interesting to run field-cycling experiments to measure T_1 and T_S over**
247 **a larger ranges of magnetic fields so to figure out the CSA contribution, but this would require a fast**
248 **sample shuttle coupled to a fluorine probe, currently not available in our laboratory. A second generation**
249 **molecular core might be a better candidate to investigate the underlining relaxation mechanisms.** The lack
250 of endogenous ^{19}F in the human body and the high sensitivity achievable in ^{19}F NMR mean that singlet
251 spin order prepared on ^{19}F spin pairs has potentially far reaching applications in the field of magnetic
252 resonance imaging and molecular tracing.

5 ADDITIONAL REQUIREMENTS

CONFLICT OF INTEREST STATEMENT

253 CE is an employee of Magritek GmbH. The authors declare that the research was conducted in the absence
254 of any commercial or financial relationships that could be construed as a potential conflict of interest.

AUTHOR CONTRIBUTIONS

255 GP: conceptualization, methodology development, NMR experiments, analysis, writing-review and editing.
256 ST: conceptualization, chemical design and synthesis, writing-review and editing. CE: pulse sequences
257 on Magritek, engineering and software. DY: chemical synthesis, characterisation and analysis. GJT: x-ray
258 diffraction and analysis.

FUNDING

259 Financial support was provided by EPSRC UK grant numbers EP/V047663/1, EP/X525807/1 and
260 EP/W021129/1.

ACKNOWLEDGMENTS

261 The authors would like to thank Dr. N. J. Wells for providing access to the 400 MHz NMR spectrometer
262 equipped with a fluorine probe.

SUPPLEMENTAL DATA

263 The Supplementary Material for this article can be found online at: ...

REFERENCES

- 264 1 .Saika A, Gutowsky HS. An unusual fluorine magnetic resonance multiplet. *Journal of the American*
265 *Chemical Society* **78** (1956) 4818–4819. doi:10.1021/ja01599a081.
- 266 2 .Petrakis L, Sederholm CH. NMR Fluorine-Fluorine Coupling Constants in Saturated Organic
267 Compounds. *The Journal of Chemical Physics* **35** (1961) 1243–1248. doi:10.1063/1.1732030.
- 268 3 .Servis KL, Fang KN. Nuclear magnetic resonance studies of ^{19}F - ^{19}F spin-spin coupling. 1-substituted
269 4,5-difluoro-8-methylphenanthrenes. *Journal of the American Chemical Society* **90** (1968) 6712–6717.
270 doi:10.1021/ja01026a027.
- 271 4 .Mallory FB, Mallory CW, Fedarko MC. Substituent effects on through-space fluorine-19-fluorine-19
272 coupling in the 1,8-difluoronaphthalene system. *Journal of the American Chemical Society* **96** (1974)
273 3536–3542. doi:10.1021/ja00818a029.
- 274 5 .Mallory FB, Mallory CW, Ricker WM. Nuclear spin-spin coupling via nonbonded interactions. 4.
275 fluorine-fluorine and hydrogen-fluorine coupling in substituted benzo[c]phenanthrenes. *The Journal of*
276 *Organic Chemistry* **50** (1985) 457–461. doi:10.1021/jo00204a006.
- 277 6 .Bakhmutov VI, Galakhov MV, Fedin EI. Through-space ^{19}F , ^{19}F spin—spin coupling constants in
278 some fluoroallyl cations. *Magnetic Resonance in Chemistry* **23** (1985) 971–972. doi:10.1002/mrc.
279 1260231117.
- 280 7 .Ernst L, Ibrom K, Marat K, Mitchell RH, Bodwell GJ, Bushnell GW. syn-ar,ar'-
281 difluorometacyclophanes: Strong ^{19}F , ^{19}F spin-spin interactions transmitted through space. *Chemische*
282 *Berichte* **127** (1994) 1119–1124. doi:https://doi.org/10.1002/cber.19941270623.
- 283 8 .Ernst L, Ibrom K. A new quantitative description of the distance dependence of through-space ^{19}F , ^{19}F
284 spin-spin coupling. *Angewandte Chemie International Edition in English* **34** (1995) 1881–1882.
285 doi:https://doi.org/10.1002/anie.199518811.
- 286 9 .Mallory FB, Mallory CW, Grant DM, Harris RK, editors, *Encyclopedia of Nuclear Magnetic Resonance*
287 (J. Wiley & Sons), vol. 3 (1996), 1491–1501.
- 288 10 .Mallory FB, Mallory CW, Butler KE, Lewis MB, Xia AQ, Luzik ED, et al. Nuclear spinspin coupling
289 via non-bonded interactions. 8.1 the distance dependence of through-space fluorinefluorine coupling.
290 *Journal of the American Chemical Society* **122** (2000) 4108–4116. doi:10.1021/ja993032z.
- 291 11 .Vasos PR, Comment A, Sarkar R, Ahuja P, Jannin S, Ansermet JP, et al. Long-lived states to sustain
292 hyperpolarized magnetization. *Proceedings of the National Academy of Sciences* **106** (2009) 18469–
293 18473. doi:10.1073/pnas.0908123106.
- 294 12 .Pileio G, Bowen S, Laustsen C, Tayler MCD, Hill-Cousins JT, Brown LJ, et al. Recycling and imaging
295 of nuclear singlet hyperpolarization. *Journal of the American Chemical Society* **135** (2013) 5084–5088.
296 doi:10.1021/ja312333v.

- 297 **13**. Kiryutin AS, Rodin BA, Yurkovskaya AV, Ivanov KL, Kurzbach D, Jannin S, et al. Transport
298 of hyperpolarized samples in dissolution-dnp experiments. *Phys. Chem. Chem. Phys.* **21** (2019)
299 13696–13705. doi:10.1039/C9CP02600B.
- 300 **14**. Salvi N, Buratto R, Bornet A, Ulzega S, Rentero Rebollo I, Angelini A, et al. Boosting the sensitivity
301 of ligand-protein screening by nmr of long-lived states. *Journal of the American Chemical Society* **134**
302 (2012) 11076–11079. doi:10.1021/ja303301w.
- 303 **15**. Sarkar R, Vasos PR, Bodenhausen G. Singlet-state exchange nmr spectroscopy for the study of
304 very slow dynamic processes. *Journal of the American Chemical Society* **129** (2007) 328–334.
305 doi:10.1021/ja0647396.
- 306 **16**. Cavadini S, Dittmer J, Antonijevic S, Bodenhausen G. Slow diffusion by singlet state nmr spectroscopy.
307 *Journal of the American Chemical Society* **127** (2005) 15744–15748. doi:10.1021/ja052897b.
- 308 **17**. Dumez JN, Hill-Cousins JT, Brown RC, Pileio G. Long-lived localization in magnetic resonance
309 imaging. *Journal of Magnetic Resonance* **246** (2014) 27–30. doi:https://doi.org/10.1016/j.jmr.2014.06.
310 008.
- 311 **18**. Pileio G, Dumez JN, Pop IA, Hill-Cousins JT, Brown RC. Real-space imaging of macroscopic
312 diffusion and slow flow by singlet tagging mri. *Journal of Magnetic Resonance* **252** (2015) 130–134.
313 doi:https://doi.org/10.1016/j.jmr.2015.01.016.
- 314 **19**. Pileio G, Ostrowska S. Accessing the long-time limit in diffusion nmr: The case of singlet assisted
315 diffusive diffraction q-space. *Journal of Magnetic Resonance* **285** (2017) 1–7. doi:https://doi.org/10.
316 1016/j.jmr.2017.10.003.
- 317 **20**. Tourell MC, Pop IA, Brown LJ, Brown RCD, Pileio G. Singlet-assisted diffusion-nmr (sad-nmr):
318 redefining the limits when measuring tortuosity in porous media. *Phys. Chem. Chem. Phys.* **20** (2018)
319 13705–13713. doi:10.1039/C8CP00145F.
- 320 **21**. Melchiorre G, Giustiniano F, Rathore S, Pileio G. Singlet-assisted diffusion-nmr (sad-nmr): extending
321 the scope of diffusion tensor imaging via singlet nmr. *Frontiers in Chemistry* **11** (2023). doi:10.3389/
322 fchem.2023.1224336.
- 323 **22**. Korenchan D, Lu J, Sabba M, Dagys L, Brown L, Levitt M, et al. Limits of the quantum cognition
324 hypothesis: ³¹P singlet order lifetimes of pyrophosphate from experiment and simulation. *ChemRxiv*
325 (2022). doi:https://doi.org/10.26434/chemrxiv-2022-7cvbc-v2.
- 326 **23**. Harbor-Collins H, Sabba M, Bengs C, Moustafa G, Leutzsch M, Levitt MH. NMR spectroscopy of
327 a ¹⁸O-labeled rhodium paddlewheel complex: Isotope shifts, ¹⁰³Rh–¹⁰³Rh spin–spin coupling, and
328 ¹⁰³Rh singlet NMR. *The Journal of Chemical Physics* **160** (2024) 014305. doi:10.1063/5.0182233.
- 329 **24**. Dolbier WRJ (John Wiley Sons, Ltd) (2016). doi:https://doi.org/10.1002/9781118831106.
- 330 **25**. Murai T, Xing Y, Kurokawa M, Kuribayashi T, Nikaido M, Elboray EE, et al. One-pot preparation of
331 (nh)-phenanthridinones and amide-functionalized [7]helicene-like molecules from biaryl dicarboxylic
332 acids. *The Journal of Organic Chemistry* **87** (2022) 5510–5521. doi:10.1021/acs.joc.1c02769.
- 333 **26**. Hahn EL. An accurate nuclear magnetic resonance method for measuring spin-lattice relaxation times.
334 *Phys. Rev.* **76** (1949) 145–146. doi:10.1103/PhysRev.76.145.
- 335 **27**. Pileio G. Singlet nmr methodology in two-spin-1/2 systems. *Progress in Nuclear Magnetic Resonance*
336 *Spectroscopy* **98-99** (2017) 1–19. doi:https://doi.org/10.1016/j.pnmrs.2016.11.002.
- 337 **28**. Elliott SJ, Bengs C, Brown LJ, Hill-Cousins JT, O’Leary DJ, Pileio G, et al. Nuclear singlet relaxation
338 by scalar relaxation of the second kind in the slow-fluctuation regime. *The Journal of Chemical Physics*
339 **150** (2019) 064315. doi:10.1063/1.5074199.
- 340 **29**. Pileio G. Singlet state relaxation via scalar coupling of the second kind. *The Journal of Chemical*
341 *Physics* **135** (2011) 174502. doi:10.1063/1.3651479.

- 342 **30** .Pileio G. Singlet state relaxation via intermolecular dipolar coupling. *The Journal of Chemical Physics*
343 **134** (2011) 214505. doi:10.1063/1.3596379.
- 344 **31** .Pileio G, Levitt MH. J-stabilization of singlet states in the solution nmr of multiple-spin systems.
345 *Journal of Magnetic Resonance* **187** (2007) 141–145. doi:https://doi.org/10.1016/j.jmr.2007.03.019.
- 346 **32** .Gerig JT. Fluorine nmr (2001). doi:https://api.semanticscholar.org/CorpusID:20942460.
- 347 **33** .Pileio G, Levitt MH. Theory of long-lived nuclear spin states in solution nuclear magnetic resonance.
348 II. Singlet spin locking. *The Journal of Chemical Physics* **130** (2009) 214501. doi:10.1063/1.3139064.
- 349 **34** .Ahuja P, Sarkar R, Vasos PR, Bodenhausen G. Molecular properties determined from the relaxation of
350 long-lived spin states. *The Journal of Chemical Physics* **127** (2007) 134112. doi:10.1063/1.2778429.
- 351 **35** .Pileio G, Hill-Cousins JT, Mitchell S, Kuprov I, Brown LJ, Brown RCD, et al. Long-lived nuclear
352 singlet order in near-equivalent ¹³C spin pairs. *Journal of the American Chemical Society* **134** (2012)
353 17494–17497. doi:10.1021/ja3089873.
- 354 **36** .Stevanato G, Hill-Cousins JT, Häkansson P, Roy SS, Brown LJ, Brown RCD, et al. A nuclear singlet
355 lifetime of more than one hour in room-temperature solution. *Angewandte Chemie International*
356 *Edition* **54** (2015) 3740–3743. doi:https://doi.org/10.1002/anie.201411978.